Characterization and photoelectrochemical properties of chemical bath deposited n-PbS thin films

M. A. BAROTE*, A. A. YADAV[a], T. V. CHAVAN[a], E. U. MASUMDAR[a]
Department of Physics, Azad college, Ausa-413520, Maharashtra, India
[a]Thin Film Research Laboratory, Department of Physics, Rajarshi Shahu Mahavidyalaya, Latur-413512, Maharashtra, India

Lead sulphide thin films have been deposited on amorphous and fluorine doped tin oxide (FTO) coated glass substrates using simple and inexpensive chemical bath deposition technique. The reactive substances used to obtain the PbS thin films were lead sulphate, thiourea and sodium hydroxide. Triethanolamine (TEA) was used as a complexing agent. The 'as-deposited' films were characterized for structural, morphological, compositional, optical, electrical and photoelectrochemical (PEC) properties. The X-ray diffraction (XRD) studies reveal that the films are polycrystalline in nature with cubic phases. The energy dispersive analysis by X-ray (EDAX) shows that films are Pb rich. The surface morphology and crystallite size were determined by scanning electron microscope measurements. The optical studies were carried out from spectroscopy measurements in the wavelength range 350-3300 nm. The band gap energy is estimated as 0.49 eV. The film shows n-type conduction mechanism. The photoelectrochemical cell with PbS film as a photo anode and sulphide-polysulphide (1M) solution as an electrolyte is constructed and investigated for various cell parameters. The solar to electrical conversion efficiency (η) and fill factor (FF) are found to be 0.041 % and 36.8% respectively.

(Received March 25, 2011; accepted April 11, 2011)

Keywords: PbS thin films, Chemical bath deposition, XRD, EDAX, SEM

1. Introduction

Semiconductor materials are always in focus due to their outstanding electronic and optical properties and potential applications in various devices including light-emitting diodes [1], single electron transistors and field effect transistors [2]. The electronic and optical properties of semiconductor materials can be changed by changing their size and shapes [3]. As an important IV-VI group semiconductor, lead sulphide (PbS) is an important direct narrow band gap semiconductor material (≈ 0.41 eV at room temperature) [4], and has been widely used in many fields such as Pb^{2+} ion-selective sensors [5], IR detector [6], photography [7] and solar absorption [8]. Due to the non-linear optical properties PbS nanoparticles has found an extensive applications in optical devices such as optical switch [9]. In addition PbS has been utilized as photo resistance, diode lasers, humidity and temperature sensors, decorative and solar control coatings [10-11]. In recent years, many researchers have been studied PbS thin film properties for various nanodevice applications. Dan Li [12] studied the nonlinear optical properties of PbS nanoparticles. Nanda [13] investigated the band-gap tuning of PbS nanoparticles. Muscat [14] studied the surface of galena PbS using the first-principles calculations. Sushil Kumar [15] reported the characterization of vacuum evaporated PbS thin films. Preobrajenski [16] reported the atomic and electronic structure of epitaxial lead sulfide on InP [17] synthesized and characterized the lead sulfide nanorods and nanowires. Gaiduk [18] deposited PbS films on Si, Ge and GaAs substrate. Badr [19] investigated the effect of PbS shell on the optical and electrical properties of PbSe core nanoparticles.

These films can be obtained by several methods such as electrodeposition [20], spray pyrolysis [21], photoaccelerated chemical deposition [10], microwave heating [22] and chemical bath deposition (CBD) [23-24]. Among these methods chemical bath deposition is just one of the more utilized due to its low cost, the quality of the films and convenience for large area deposition.

In the present investigation, we have obtained PbS thin films in alkaline medium and their structural, morphological, optical, electrical and photo-electrochemical properties have been studied.

2. Experimental details

2.1. Synthesis of Lead sulphide thin films

The Pbs thin films were grown on an amorphous and FTO-coated glass substrates. The deposition was done in a reactive solution prepared in a 250 ml beaker containing equimolar solutions of lead sulphate and thiourea. TEA was used as a complexing agent and pH of the reaction mixture was adjusted to about 10.5 ± 0.1 with the help of NaOH and ammonia solution. Thoroughly cleaned glass substrates were mounted on specially designed substrate holder and rotated with constant speed in the reaction mixture. To obtain good quality samples the time, temperature and speed of the rotation were optimized. These optimized parameters were 60 min., 80 ^{0}C, and 65 ±

2 rpm respectively. After deposition substrates were subsequently taken out of the chemical bath, rinsed with bidistilled water, dried and placed into desiccators.

2.2. Characterization techniques

The film thickness was measured by gravimetric weight difference method using sensitive microbalance. X-ray diffraction pattern of the 'as-deposited' film was recorded with Philips PW-3710 X-ray diffractometer in the scanning range of 2θ from 20-80^0 with Cu-k_α (λ = 1.5406 Å) radiations. The surface morphology and composition was studied by scanning electron microscopy (SEM) and energy dispersive analysis by X-ray (EDAX) with the help of JEOL-JSM 5600 Japan. The optical absorption studies were carried out using UV-VIS-NIR spectrophotometer (Carry-5000 Japan) in the 350-3300 nm wavelength range. Electrical resistivity and thermo-emf measurements were done using DC two probe press contact method in the temperature range 300-500 K.

2.3. Fabrication of PEC solar cell

Photoelectrochemical cell was fabricated using the 'as- deposited' PbS thin film on FTO-coated glass substrate as an active photo electrode, graphite rod as an counter electrode and the saturated calomel electrode (SCE) as a reference electrode. The aqueous 1 M polysulphide (Na_2S + S + NaOH) was used as a redox electrolyte. These three electrodes were fitted in the bakelite holder. A 100 W tungsten filament lamp (intensity 25 mW/cm^2) was used as a light source. To avoid direct heating of cell, water lens was interposed between the lamp and the cell. The distance between the photoelectrode and counter electrode was 0.2 cm. The area of the semiconducting thin film other than that in contact with electrolyte was covered by epoxy resin to annul any contribution due to the contact of the base contact oxide material with the electrolyte and its interference in the measured values of the net photocurrent density. For measurement of the power output characteristics, a two electrode configuration consisting of the thin film photoelectrode and graphite as the counter electrode was used. Measurements for the power output characteristics and I–V plots were made at fixed intervals after waiting for sufficient time to equilibrate the system at that setting (both in dark as well as under illumination). The logs I against V plots are used to calculate the junction ideality factor in dark and under illumination. Various currents and voltages were measured by the 6½ digit, HP-34401. Mott–Schottky plots were plotted using as LCR (Aplab model 4912) at built in frequency 1 kHz.

3. Results and discussion

3.1. Kinetic studies

The rate of PbS thin film growth is mostly dependent on the rate of release of Pb^{2+} and S^{2-} ions from the complex bound state. This is achieved by controlled precipitation of PbS in the reaction bath. The solubility product of PbS is very small (≈10^{-28}), the precipitation is controlled by controlling the concentration of free Pb^{2+} ions in the chemical bath. In this case triethanolamine is used as the complexing agent, which releases a small concentration of ions. The chemical reaction for the deposition of PbS by chemical bath deposition is given by

$$SC(NH_2)_2 + OH^- = CH_2N_2 + H_2O + HS^- \quad (1)$$

$$HS^- + OH^- = H_2O + S^{2-} \quad (2)$$

$$Pb^{2+} + S^{2-} = PbS \quad (3)$$

It is observed that growth rate of PbS thin film is dependent upon the concentration of the ion in the bath. The molar concentrations of initial ingredients used for deposition of PbS was between 0.25 to 1.25 M. We observed that film thickness is increased with increase in molar concentration up to 1M and then it decreases for further increase in the concentration of basic ingredients as shown in Fig. 1. The effect of deposition temperature and time on the growth rate of film has been studied. It is found that at room temperature no film formation was observed. The reason is that, at low temperature almost all the metal ions are in complex-bound state. So, the temperature of reaction counter was increased from 30 to 90 ^{0}C to get homogeneous and adherent PbS thin films. Fig. 2. shows the variation of film thickness with temperature. It is observed that film thickness increases almost linearly with increase in temperature but at higher temperature homogeneous precipitation formed very early and which affect on the film growth [25-26]. So, for uniform deposition of PbS thin film at 80 ^{0}C temperature was considered to be optimized. Fig. 3 shows the plot of film thickness against the deposition time. It is seen that film growth is linear with time but at longer deposition time there is no significant growth in the film thickness. This is due to the fact that at longer deposition time the reaction in the bath is to be completed and then after that there is absence of Pb^{2+} and S^{2-} ions, so the optimized deposition time is 60 min. The film thickness of PbS is measured by gravimetric weight difference method using sensitive microbalance is found to be 1378 nm.

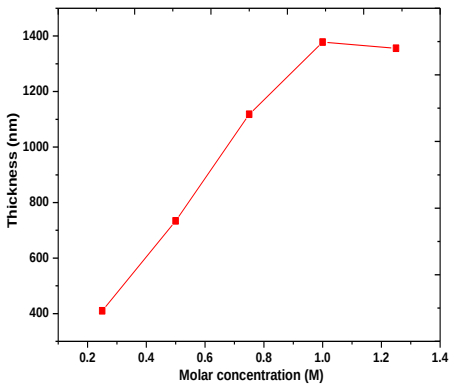

Fig. 1. Variation of film thickness with molar concentration for chemically deposited PbS thin film.

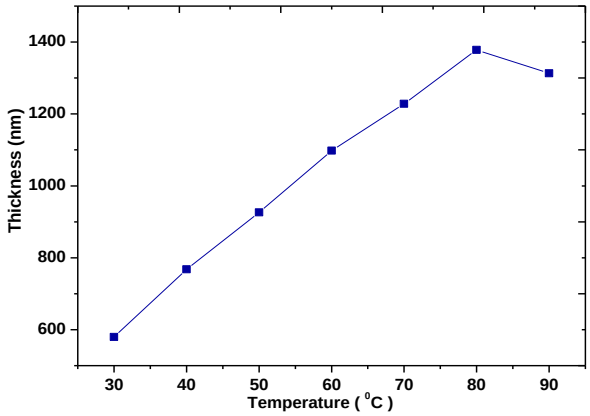

Fig. 2. Variation of film thickness with deposition temperature for chemically deposited PbS thin film.

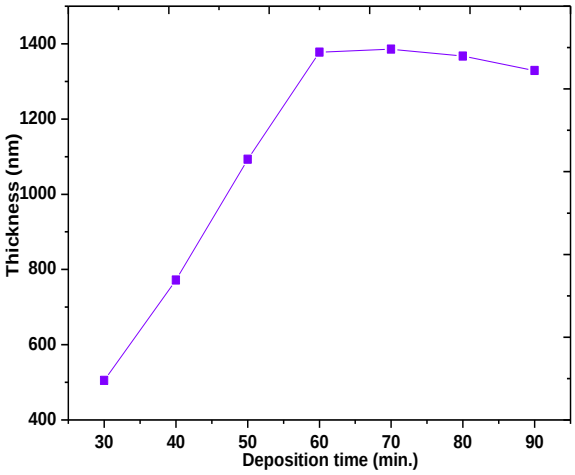

Fig. 3. Variation of film thickness with deposition time for chemically deposited PbS thin film.

3.2. Structural analysis

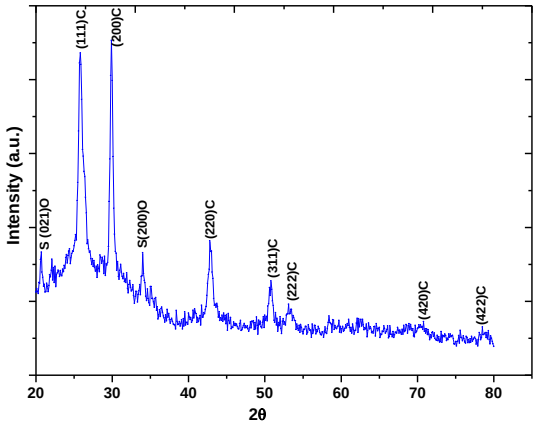

Fig. 4. X-ray diffractogram of chemically deposited PbS thin film.

A typical XRD pattern of the 'as-deposited' PbS thin film on glass substrate is shown in Fig. 4. It shows several diffraction peaks at 2θ values of 25.88^0, 29.96^0, 42.86^0, 50.88^0, 53.19^0, 70.86^0 and 78.56^0. These were assigned to the diffraction lines produced by (1 1 1), (2 0 0), (2 2 0), (3 1 1), (2 2 2), (4 2 0) and (4 2 2) planes of the face-centered cubic (fcc) structure of PbS. The dominant and sharp peaks indicate that PbS nanocrystals are highly crystalline. The lattice constant for cubic phase is determined by using the relation

$$a = d\,(h^2 + k^2 + l^2)^{1/2} \quad (4)$$

The lattice constant calculated from the above relation is found to be a = 5.961 Å, which is almost in agreement with the standard data from JCPDS card No. 78-1901 (a = 5.931 Å). The impurities like elemental S, and PbO_2 were detected in the XRD pattern. The presence of oxide phases can be attributed to excess Pb which can be regarded as being $Pb(OH)_2$ or PbO due to pH value larger than 10, while excess S excess S exist in the form of elemental S arising from extraneous decomposition of S ions at higher concentrations [27].

The average grain size of the film was calculated using Scherrer's formula

$$D = k\lambda / \beta\cos\theta \quad (5)$$

Where k is constant 0.94, λ is the wavelength of X-ray, β is full width at half the peak maximum in radians and θ is found to be 7.5 nm.

3.3. Surface morphology and EDAX analysis

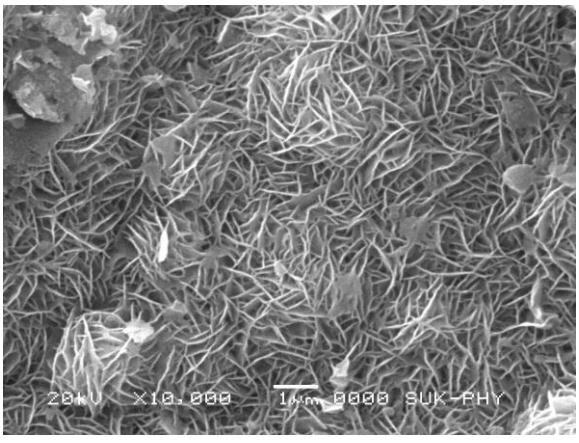

Fig. 5. SEM micrograph of chemically deposited PbS thin film.

The surface morphology of thin film was determined by scanning electron microscopy (SEM). Fig. 5 shows the SEM image of the PbS thin film at 10,000 x magnifications. The growth of the film was observed to be a mesh-like structure overgrown on the uniformly distributed grains of PbS, that looks like a leafy cabbage-type structure [28]. This can be partially justified by the nucleation of fresh PbS molecules over the grown

molecules during the growth process. The average grain size observed was 100 nm. The increase in grain size may be due to fusion of grains to form cluster type structure.

The energy-dispersive analysis by X-ray has been used to determine the composition of PbS thin film. The analysis confirms the presence of Pb and S in the deposited film with Pb ≈ 60.95 and S ≈ 39.05. It confirms that the films are lead (Pb) rich. The possible composition and structure of chemically deposited PbS thin films can vary widely may be due to the variation of pH value and due to the presence of reducing agent such as sulphate in the reaction mixture [29].

3.4. Optical properties

The optical absorption spectra of chemically deposited PbS thin film sample at room temperature was studied by UV-VIS-NIR double beam spectrophotometer in the range 350-3300 nm without taking into account the reflection and transmission losses. The optical absorption is characterized the relation between the absorption coefficient (α) and the photon energy (hυ) for different allowed transition as

$$.\alpha h\upsilon = A\,(h\upsilon - E_g)^n \qquad (6)$$

where α is the absorption coefficient, hυ the photon energy, E_g the optical band gap and A is the constant which is related to the effective masses associated with the valance band and conduction band [30] and n has the significance of an electronic transition, usually ½ for allowed direct transition and 3/2, 2 and 3 for allowed indirect, forbidden direct and forbidden indirect transitions, respectively. It is possible to determine nature of transition involved by plotting the graph of $(\alpha h\upsilon)^2$ versus hυ. The plot of $(\alpha h\upsilon)^2$ versus hυ is shown in Fig.6.

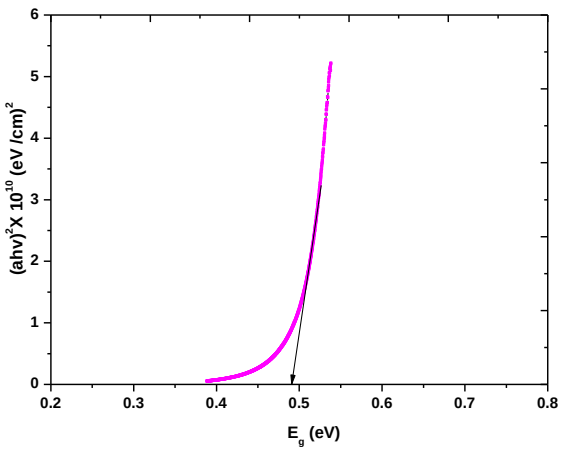

Fig. 6. Plot of (αhυ)2 versus hυ for chemically deposited PbS thin film.

The energy band gap can be obtained by extrapolating the straight-line portion of graph to zero absorption coefficient. The band energy is found to be 0.49 eV which is slightly different than the bulk material (0.41 eV). This may be due to the fact that the amorphous or nanocrystalline films show band gap energies higher that those of the corresponding bulk materials. The increase in the band gap energy is due the nano-crystalline nature of the PbS film [31-32].

3.5. Electrical resistivity

The dark electrical resistivity of 'as-deposited' PbS film was measured using dc two point press contact method, in the temperature range 300-500 K. The variation of log ρ with reciprocal temperature (1000/K) is depicted in Fig. 7. The electrical resistivity at room temperature is found to be of the order of 10^5 Ω-cm, which is in good agreement with reported value by Gadve et al. [33]. It can be observed that electrical resistivity has two linear portions, first in the lower temperature range (300-375 K) and second in the higher temperature range (375-500 K). The high value of resistivity may be attributed due to nanocrystallanity of the film, grain boundary discontinuities and presence of surface states [34]. The decrease in resistivity with increase in temperature confirmed semiconductor nature of PbS thin film.

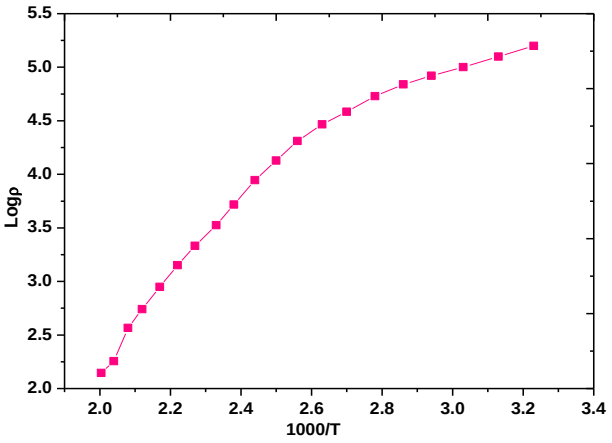

Fig. 7. Variation of log ρ with reciprocal of temperature for chemically deposited PbS thin film.

The activation energies were calculated using the relation

$$\rho = \rho_0 \exp(-E_a / kT) \qquad (7)$$

Where ρ is the resistivity at temperature T, ρ_0 is a constant, k is the Boltzmann constant, T is absolute temperature and E_a is the activation energy. The activation energy represents location of trap levels below the conduction band. The activation energies for 'as-deposited' film are 0.212 eV and 0.976 eV for low and high temperature regions, respectively. The type of conductivity exhibited by chemical bath deposited PbS thin film is determined by thermoelectric power (TEP) measurement the TEP depends on the location of Fermi energy level in the material and the type of scattering mechanism [35]. From the sign of the terminal connected towards hot end it can

be deduced the sign of the predominant charge carriers. In our case the hot end is connected to the positive terminal, the film shows n-type conductivity. The vacancies and interstitials control the conductivity type, an excess of Pb causes n-type conductivity [36].

3.6. Photoelectrochemical (PEC) solar cell studies

3.6.1 Current-voltage characteristics

The current voltage characteristics of 'as-deposited' PbS thin film is studied in the voltage range of ± 1 V, in dark and under light illumination. It is observed that the forward current increases rapidly with applied voltage. The increase in forward current can be attributed to the small contact height and increase in tunneling mechanism [37]. Fig. 8 shows I-V characteristics in the dark and under light illumination. The junction ideality factor is calculated using famous diode equation

$$I = I_0 (e^{qv/nkT} - 1) \quad (8)$$

where n is junction ideality factor, I_0 is the reverse saturation current, V is the forward bias voltage and I is the forward current in dark. The junction ideality factor n_l and n_d are determined to be 2.28 and 3.27. The n values are found to be higher than the ideal value, it is a common fact found in many polycrystalline photoelectrode materials [38].

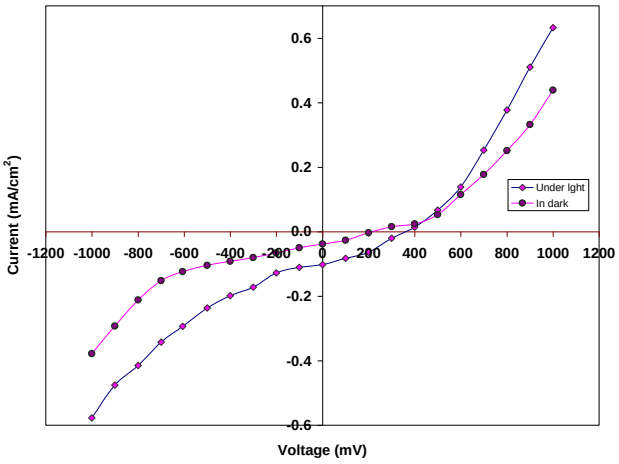

Fig. 8. Current voltage characteristics of chemically deposited PbS thin film.

3.6.2. Power output characteristics

Photoelectrochemical cell was fabricated using PbS thin film as the active photoelectrode and graphite as a counter electrode. Typical photocurrent density versus photovoltage characteristics of PbS film / polysulphide under the illumination is shown in Fig. 9. The fill factor (FF) is evaluated from the relation

$$FF = V_m \times I_m \; / \; V_{oc} \times I_{sc} \quad (9)$$

Where the I_m and V_m are the values of maximum current and maximum voltage. The efficiency η (%) is calculated from the relation

$$\eta = V_{oc} \times I_{sc} \times FF \times 100 / P_{input} \quad (10)$$

Where P_{input} is the input light energy. The series resistance (R_s) and shunt resistance (R_{sh}) are estimated from the slope of power output characteristics at I = 0 and V = 0 respectively using the relation

$$(dI / dV)_{I=0} = (1 / R_s) \quad (11)$$
$$(dI / dV)_{V=0} = (1 / R_{sh}) \quad (12)$$

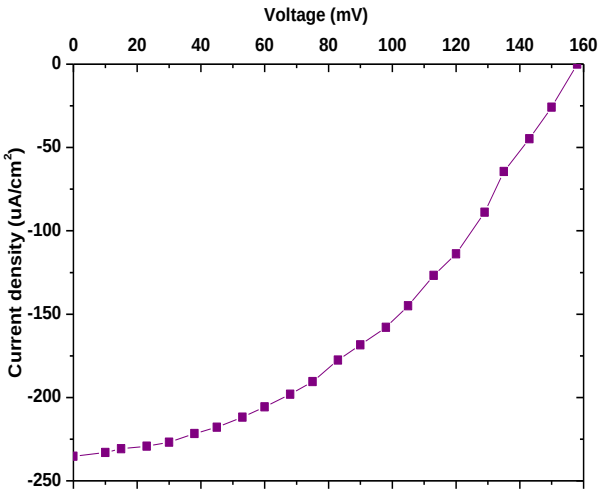

Fig. 9. Plot of power output characteristics for n-PbS / 1M (NaOH + Na_2S + S) / C PEC Cell.

The FF and power conversion efficiency is found to be 36.8% and 0.041% respectively. In general, the efficiency so far obtained with such cells is quite low, which could be attributed to the factors such as photoelectrode resistivity and light absorption by the electrolyte solution [39]. The series and shunt resistances are calculated as 355 Ω and 2.84 kΩ respectively.

3.6.3. Mott-Schottky plots

The capacitance-voltage measurements were performed on this cell to obtain the value of flat band potential. Flat band potential is the measure of maximum open-circuit voltage attainable from the cell. It gives the information of the relative positions of the Fermi levels of the semiconductor and the electrolyte [40]. The space charge layer capacitance was measured under reverse biased condition and flat band potential is obtained from the Mott-Schottky relation [41]. The variation of $1 / C_s^2$ versus electrode potential V is shown in Fig. 10. The extrapolation on V-axis which gave a flat band potential which is equal to -0.745 V / SCE. The flat band potential is found to larger, it may be due to the higher magnitude of the photoelectrode thickness [42].

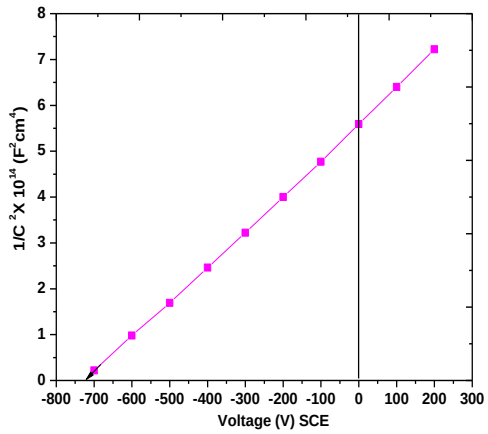

Fig. 10. Mott-Schottky plots for n-PbS / polysulphide / C photoelectrochemical cell.

4. Conclusions

In summary, polycrystalline n-PbS thin films have been synthesized by simple and economical chemical bath deposition technique. The structural studies indicate that these films are nanocrystalline in nature with cubic structure. The optical band gap of 'as-deposited' film was found to be 0.49 eV having direct band type transitions. The temperature dependence of the dc conductivity suggests that there are two types of conduction channels that contribute to the conductivity. The fill factor (FF) and conversion efficiency (η) for the n-PbS / 1M (NaOH + Na_2S + S) / C PEC cell configuration are found to be 36.8 % and 0.041 %, respectively.

References

[1] V. L. Colvin, M. C. Schlamp, A. P. Alivisatos, Nature, **370**, 354 (1994).
[2] B. A. Ridley, B. Nivi, J. M. Jacobsn, Science, **286**, 746 (1999).
[3] P. D. Yang, C. M. Lieber, Science, **273**, 1836 (1996).
[4] S. Seghaier, N. Kamoun, R. Brini, A. B. Amara, Mater. Chem. Phys. **97**, 71 (2006).
[5] H. Hirata, K. Higashiyama, Bull. Chem. Soc. Jpn. **44**, 2420 (1971).
[6] P. Gadenne, Y. Yagil, G. Deutscher, J. Appl. Phys. **66**, 3019 (1989).
[7] P. K. Nair, O. Gomezdaza, M. T. S. Nair, Adv. Mater. Opt. Electron. **1**, 139 (1992).
[8] T. K. Chaudhari, S.Chatterjes, Proc. Int. Conf. Thermo electronics, **11**, 40 (1992).
[9] R. S. Kane, R. E. Cohen, R. Silbey, J. Phys. Chem. **100**, 7928 (1996).
[10] P. K. Nair, V. M. Garcia, A. B. Hernandez, M. T. S. Nair, J. Phys. D: Appl. Phys. **24**, 1466 (1991).
[11] I. Pop, C. Nascu, V. Ionescu, E. Indrea, I. Bratu, Thin Solid Films, **307**, 240 (1997).
[12] D. Li, C. Liang, Y. Liu, S. Qian, J. Luminescence **122**, 549 (2007).
[13] K. K. Nanda, F. E. Kruis, H. Fisan, J. Appl. Phys. **91**, 2315 (2002).
[14] J. Muscat, J. D. Gale, Geochimica et Cosmochimica Acta **67**, 799 (2003).
[15] S. Kumar, T. P. Sharma, M. Zulfequar, M. Husain, Physica B **325**, 8 (2003).
[16] A. B. Preobrajenski, T. Chasse, Appl. Surface Sci. **166**, 201 (2000).
[17] T. Saraidarov, R. Reisfeld, A. Sashchiuk, Physica E **37**, 173 (2007).
[18] A. P. Gaiduk, P. I. Gaiduk, A. Nylandsted Larsen, Thin Solid Films, **516**, 3791 (2008).
[19] Y. Badr, M. A. Mahmond, Physica B **388**, 134 (2007).
[20] M. Sharon, K. S. Ramaiah, M. Kumar, M. Neumann-Spallart, C. L. Clement, Electroanal. Chem. **436**, 49 (1997).
[21] B. Thangaraju, P. Kaliannan, Semicond. Sci. Technol. **15**, 849 (2000).
[22] Y. Zhao, Xue-Hong Liao, Jian-Min Hang, Jun-Jie Zhu, Mater. Chem. Phys. **87**, 149 (2004).
[23] E. Pentia, L. Pintilie, C. Tivarus, I. Pintilie, T. Botila, Mater. Sci. Eng. B, **80**, 23 (2001).
[24] R. K. Joshi, A. Kanjilal, H. K. Sehgal, Appl. Surf. Sci. **221**, 43 (2004).
[25] D. S. Sutrave, G. S. Shahane, V. B. Patil, L. P. Deshmukh, Mater. Chem. Phys. **65**, 305 (2000).
[26] R. P. Sharma, K. C. Sharma, J. C. Garg, J. Phys. D: Appl. Phys. **24**, 2087 (1991).
[27] Y. Ueno, H. Kaigawa, T. Ohashi, T. Sugiura, H. Minoura, Solar Energy Mater. **15**, 421 (1987).
[28] L. P. Deshmukh, B. M. More, C. B. Rotti, G. S. Shahane, Mater. Chem. Phys. **45**, 145 (1996).
[29] C. Guillen, M. A. Martinez, C. Maffolte, J-Herrero, J. Elec. Soc. **148**, G602 (2001).
[30] H. M. Pathan, S. S. Kulkarni, R. S. Mane, C. D. Lokhande, Mater. Chem. Phys. **93**, 16 (2005).
[31] T. Ivanova, A. Harizanova, M. Surtchev, Mater. Lett. **55**, 327 (2002).
[32] R. S. Mane, C. D. Lokhande, Surf. Coat. Technol. **172**, 51 (2003).
[33] K. M. Gadve, S. A. Jodgudri, C. D. Lokhande, Thin Solid Films, **245**, 7 (1994).
[34] A. A. Yadav, E. U. Masumdar, J. Alloys and Compounds **505**, 787 (2010).
[35] A. A. Yadav, M. A. Barote, E. U. Masumdar, Solid State Sciences. **121**, 1173 (2010).
[36] H. Saloniemi, Academic Dissertation, VTT Pub. **423**, 32 (2000).
[37] R. Rajeshwar, R. Thompson, P. Sing, R. C. Kainthala, K. L. Chopra, J. Electrochem. Soc. **126**, 1949 (1979).
[38] L. P. Deshmukh, C. B. Rotti, K. M. Garadkar, Mater. Chem. Phys. **50**, 45 (1991).
[39] M. T. Gutierrez, J. Ortega, Sol. Energy Mater. **20**, 387 (1990).
[40] L. P. Deshmukh, G. S. Shahane, Int. J. Electron. **83**, 341 (1997).
[41] K. Y. Rajpure, C. H. Bhosale, Mater, Chem. Phys. **64**, 14 (2000).
[42] L. P. Deshmukh, P. P. Hankare, V. S. Savant, Solar Cells, **31**, 549 (1991).

*Corresponding author: barotema@yahoo.com